Available online at www.sciencedirect.com

SCIENCE DIRECT®

Coordination Chemistry Reviews 248 (2004) 603–621

COORDINATION CHEMISTRY REVIEWS

www.elsevier.com/locate/ccr

Review

Organometallic compounds with Sb–Sb or Bi–Bi bonds

L. Balázs, H.J. Breunig*

Institut für Anorganische und Physikalische Chemie, Fachbereich 2, Universität Bremen, Bremen D-28334, Germany

Received 30 July 2003

Available online 18 February 2004

Contents

Abstract

Recent developments in the chemistry of organometallic compounds with antimony–antimony or bismuth–bismuth bonds and their complexes with transition metals are reviewed in this article.

Keywords: Antimony; Bismuth; Transition metal carbonyl complexes

---

1. Introduction

The chemistry of organic derivatives of antimony and bismuth (and the other pnicogens) is related to the chemistry of carbon compounds through isolobal relations, and a large number of structures analogous to hydrocarbons are conceivable. Research in the field of the heavier pnicogens, E = Sb, Bi is however hampered by the relative weakness of both the E–C and E–E bonds, and it is often necessary to work at low temperatures in an inert atmosphere and to use sterically protecting substituents. Known structural types are shown in Scheme 1. There are various combinations of R_2E, RE and E units which lead to dimers, cyclic or chain oligomers, and bi- or polycyclic (cluster) species. The majority of these structures represent neutral molecules, but also cationic or anionic species have been synthesized. All the compounds in Scheme 1 are potential ligands that may coordinate to metal centers.

Some parts and aspects of the subject including, distibines, dibismuthines, distibenes, and dibismuthenes, organoantimony and bismuth rings have already been reviewed [1–7]. A recent review article on antimony ligands comprises also ligands with Sb–Sb bonds [8]. In the present article, the focus is laid on recent developments and a timely view is given over the whole research area. Not only compounds with Sb–C and Bi–C bonds are considered, but also related species with bonds to heavier group 14 elements and complexes with "naked" Sb_n or Bi_n ligands. The material is organised according to different types of compounds and attempts are made for a comparison of analogous systems.

---

* Corresponding author.

0010-8545/$ – see front matter © 2003 Elsevier B.V. All rights reserved.
doi:10.1016/j.ccr.2003.12.001

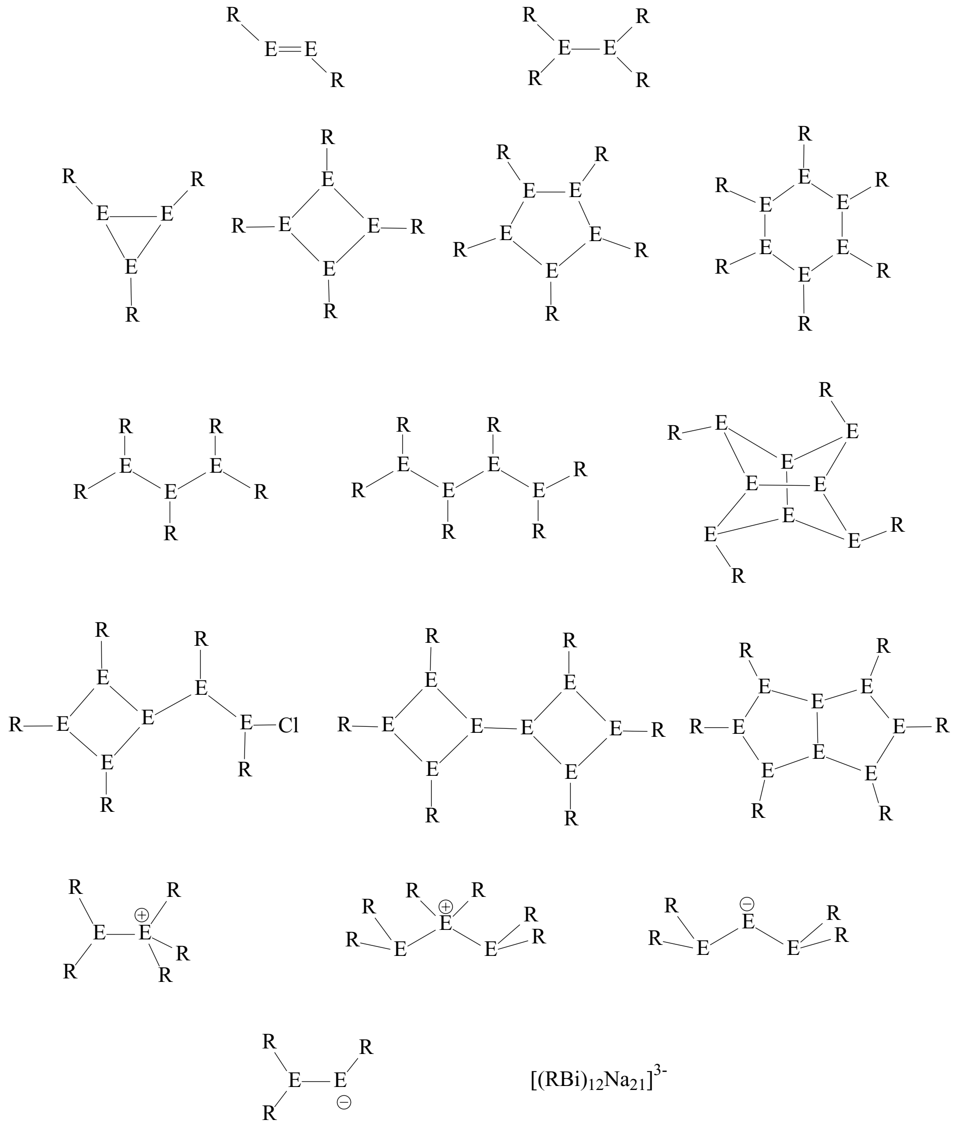

E = Sb, Bi; R = monovalent organic groups

Scheme 1.

The compounds discussed here feature Sb or Bi in the lower oxidation states between −I and +III, where fundamental differences between Bi and the lighter pnicogens can be expected. Relativistic effects should lead to a stabilization of monomeric bismuth(I) compounds with two inert electron pairs [9]. Monomers of the type RSb (stibinidenes) or RBi (bismuthinidenes) have however not been isolated in condensed phase. Only dimers and oligomers exist as stable crystalline compounds.

2. Distibenes and dibismuthenes, $(RE)_2$ (E = Sb, Bi)

Dimers of RSb or RBi are known as distibenes and dibismuthenes [6,7]. The chemistry of these heavy analogues of alkenes with double bonds between antimony or bismuth atoms has been developed by Okazaki, Tokitoh and Power using steric protection by bulky organo groups (C_6H_3-2,6-Mes_2, Mes = 2,4,6-$Me_3C_6H_2$; C_6H_3-2,6-$Trip_2$, Trip = C_6H_2-2,4,6-$^iPr_3$) [10]; Tbt = 2,4,6-$[(Me_3Si)_2CH]_3C_6H_2$ [11,12]; Bbt = {2, 4-$[(Me_3Si)_2CH]_2$-6-$(Me_3Si)_3C$}-C_6H_2 [6]) and the examples *trans*-RE=ER (E = Sb, R = Tbt [11], E = Bi, R = Tbt [12]) were synthesized and characterized by X-ray diffraction (Fig. 1). *cis*-Isomers of distibenes or dibismuthenes are not known.

A recent development is the synthesis of a stable stibabismuthene, RSb=BiR (R = Bbt) by HBr elimination from $RSbH_2$ and $RBiBr_2$ with DBU [13]. The compound was characterized by the Raman spectrum showing a strong line for the Sb–Bi stretching at 169 cm^{-1}, between the values for Sb–Sb and Bi–Bi stretching frequencies found in RSb=SbR (207 cm^{-1}, R = Tbt) and RBi=BiR (135 cm^{-1}, R = Tbt).

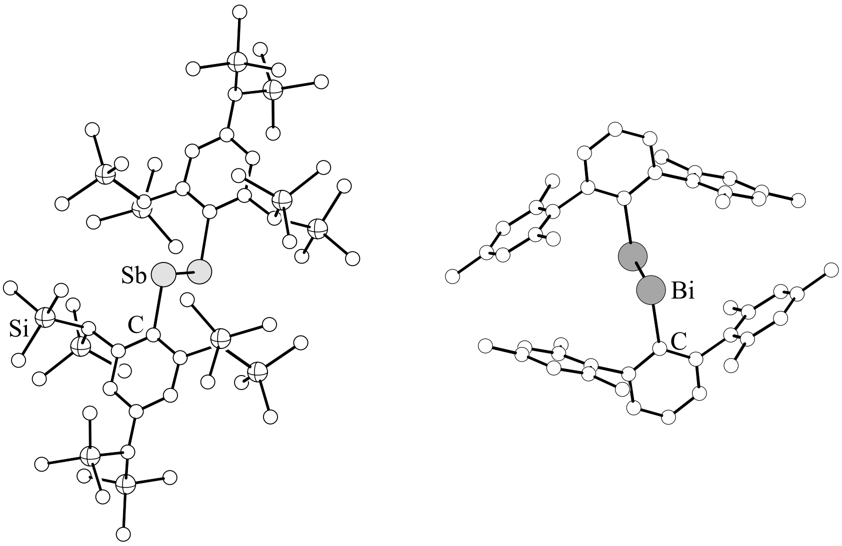

Fig. 1. Structures of the distibene TbtSb=SbTbt, Tbt = 2,4,6-[$(Me_3Si)_2CH]_3C_6H_2$ [11,12] and the dibismuthene RBi=BiR, R = 2,6-$(Me_3C_6H_2)_2C_6H_3$ [10].

Owing to disorder phenomena a complete X-ray characterization was not achieved. However, a phosphabismuthene, Mes*P=BiR (Mes* = 2, 4, 6-^{t}Bu_3-C_6H_2, R = Bbt) was recently synthesized from $RSbBr_2$ and Mes*PH_2 in the presence of DBU (DBU = 1,8-diazabicyclo[5.4.0]undec-7-ene) and characterized by X-ray diffractometry [14]. Methods used for the syntheses of Sb=Sb double bonds include the elimination of selenium from (*cyclo*-RSbSe)$_3$ (R = Tbt) with $(Me_2N)_3P$ and the dehalogenation of $RSbBr_2$ (R = Bbt) with Mg in tetrahydrofuran [6].

3. Monocyclo stibines and bismuthines, R_nE_n (n = 3–6, E = Sb, Bi)

Well defined oligomers of RSb have been studied since the 1960s, when the synthesis of (^{t}BuSb)$_4$ was published by Issleib et al. [15]. Since then various examples of cyclostibines, $(RSb)_n$ with $n = 3$–6 [1–5] have been reported. Representative structures are depicted in Fig. 2.

Trimers of the type $(RSb)_3$ (R = Me [16], Et [17], Ph [18]) have been detected by mass spectrometry in the gas phase, but only one tristibirane, i.e. *cyclo*-R_3Sb_3 [R = $(Me_3Si)_2CH$] [19] is known to exist in condensed phases. The bis(trimethylsilyl)methyl group is especially effective in the stabilization of the trimer in the *cis–trans* configuration. The unsymmetrical shape of this bulky group avoids steric hindrance between the *cis*-substituents and provides steric protection in the periphery of the ring. The tristibirane was first identified as a component of the mixture formed by the reaction of $RSbCl_2$ with Mg [20]. More recently other synthetic methods, including the reduction of $RSbCl_2$ with Li_3Sb [19], or Na/K [24], hydrogen elimination from R(H)SbSb(H)R [22] and photochemical ring contraction of R_4Sb_4 [19] or R_4Sb_8 [22] [R = $(Me_3Si)_2CH$] were reported. The *all-cis* isomer of R_3Sb_3 has not been isolated, however its formation as a ligand in a $W(CO)_5$ complex is possible [21].

Tetrastibetanes, *cyclo*-R_4Sb_4, have been synthesized more frequently and examples containing bulky substituents, R = ^{t}Bu, Cp*, $(Me_3Si)_2CH$, Mes were fully characterized. ^{t}Bu_4Sb_4 is the first cyclostibine that was characterized by single crystal X-ray diffraction [23]. Usually tetrastibetanes are folded rings and the organo groups are in *all-trans* positions. However, recently a *cis–trans* isomer of R_4Sb_4 [R = $(Me_3Si)_2CH$] was obtained as a product of the hydrogen elimination from R(H)SbSb(H)R, probably via dimerization of a distibene intermediate (Eq. (1)). An X-ray analysis revealed that the Sb_4 ring of *cis–trans* R_4Sb_4 [R = $(Me_3Si)_2CH$] is planar. This result is unexpected, because the torsion (Pitzer) strain should lead to ring folding even when steric interactions between the substituents in 1,3-positions can be ruled out.

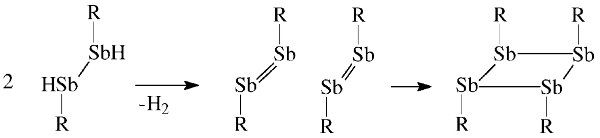

(1)

A four-membered antimony ring bearing a diantimony substituent is *cyclo*-Sb_4R_3-Sb_2R_2Cl. This ring compound was obtained by dehalogenation of $RSbCl_2$ [R = $(Me_3Si)_2CH$] with Na/K alloy in 5% yield [24]. The main product of the reduction is *cyclo*-R_3Sb_3. The structure of *cyclo*-Sb_4 R_3-Sb_2R_2Cl is depicted in Fig. 3. It consists of a folded antimony-four-ring with three $(Me_3Si)_2CH$ groups and one SbR–SbR–Cl fragment as substituents in *all-trans*-positions. The fold angles are 115.5 and 117.3°. There is a close intramolecular contact between one of the ring antimony atoms and an antimony atom of the side chain bearing the

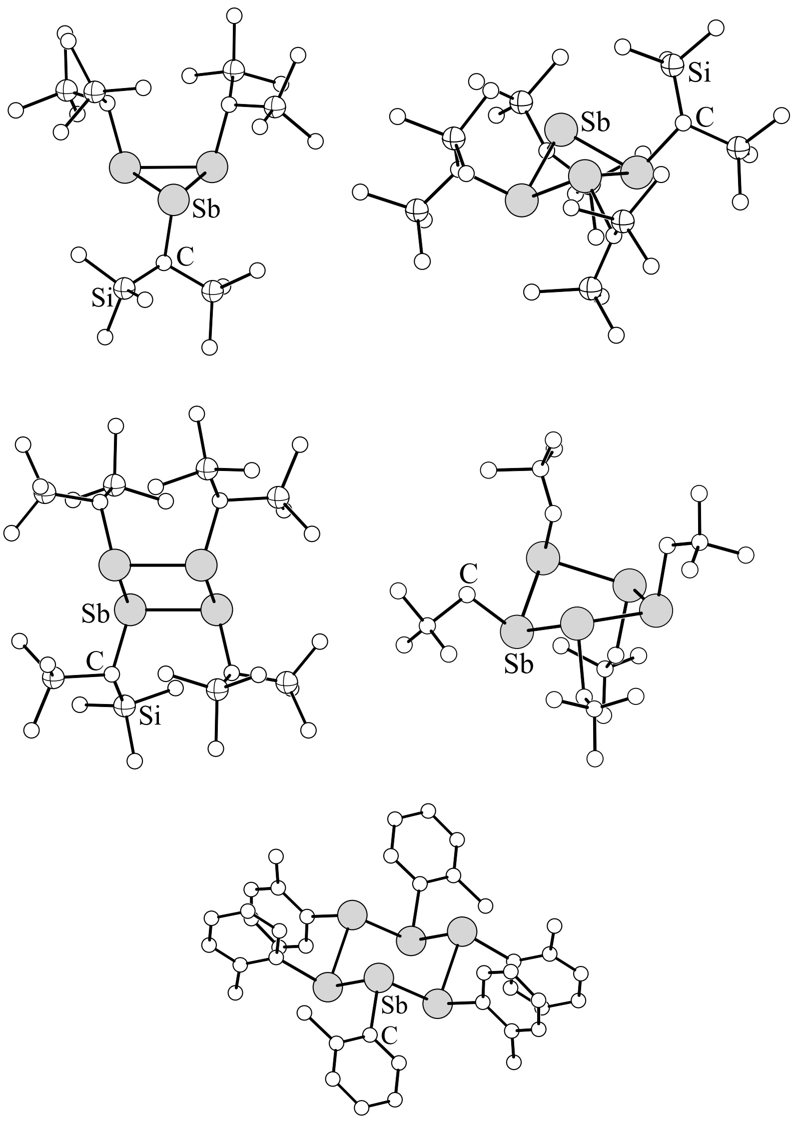

Fig. 2. Structures of *cyclo*-$(RSb)_n$ oligomers ($n = 3$–4, $R = (Me_3Si)_2CH$; $n = 5$, $R = Me_3CCH_2$; $n = 6$, R = *o*-Tol) [1,2,22,26,29].

Cl atom (Sb···Sb 3.554(2) Å) and the angle Sb···Sb–Cl is 166.17(2)°. The NMR spectra show that in solution two isomers are present. The most straight-forward interpretation is to assume that the other isomer is formed by rotation about the Sb(3)–Sb(2) bond leading to an Sb(4)···Sb(1) contact (Eq. (2)).

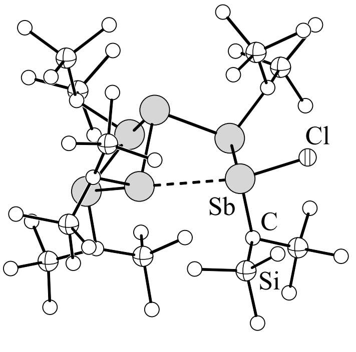

Fig. 3. Structure of *cyclo*-Sb_4R_3-Sb_2R_2Cl, $R = (Me_3Si)_2CH$ [24].

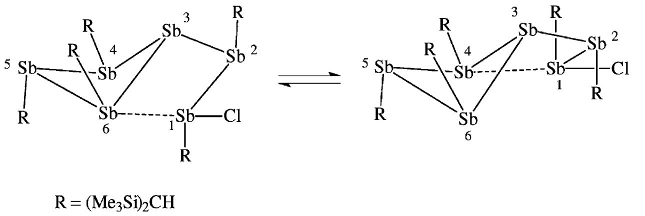

(2)

Structural data of tetrastibetanes, *cyclo*-R_4Sb_4 are given in Table 1.

Pentastibolanes, *cyclo*-R_5Sb_5 exist with less bulky alkyl or aryl substituents (R = Et, *n*-Pr, Me_3SiCH_2, Ph, Tol [2]). They are labile compounds taking part in ring–ring equilibria with tetramers in solution. Attempts to fully characterize

Table 1
Geometric parameters of tetrastibetanes

Compound	Molecular data (Å; °)		Fold angles, Sb_3–Sb_3	Space group	References
$^{t}Bu_4Sb_4$	Sb–Sb	2.814(2)–2.821(7)	132.7	$P2_1/c$	[23]
	Sb–C	2.199(2)–2.227(2)	132.8		
	Sb–Sb–Sb	84.8(1)–85.2(1)			
$Cp^*_4Sb_4$	Sb–Sb	2.836(1)		I-4	[25]
	Sb–C	2.26			
	Sb–Sb–Sb	76.7(1)			
$Cp^*_4Sb_4$	Sb–Sb	2.856(1)	144	$I41/amd$	[26]
	Sb–C	2.252(1)			
	Sb–Sb–Sb	87.1(1)			
Mes_4Sb_4	Sb–Sb	2.853(1)–2.855(1)	119.8(1)	$P\bar{1}$	[17]
	Sb–C	2.169(4)–2.186(4)	125.2		
	Sb–Sb–Sb	76.91(2)–88.10(2)			
all-trans-R_4Sb_4 ($R = (Me_3Si)_2CH$)	Sb–Sb	2.822(1)–2.878(1)	115.27(2)	$P\bar{1}$	[27]
	Sb–C	2.226(4)–2.232(4)	115.48(2)		
	Sb–Sb–Sb	80.14(2)–80.75(1)			
cis-trans-R_4Sb_4 ($R = (Me_3Si)_2CH$)	Sb–Sb	2.860(3)–2.893(4)	180	$P\bar{1}$	[22]
	Sb–C	2.19(5)–2.21(5)			
	Sb–Sb–Sb	87.88(11)–92.12(11)			
$Sb_4R_3Sb_2R_2Cl$ ($R = (Me_3Si)_2CH$)	Sb–Sb	2.8367(12)–2.8718(12)	144.2	$P\bar{1}$	[24]
	Sb–C	2.194(7)–2.223(8)	146.1		
	Sb–Sb–Sb	84.12(3)–93.32(4)			
Sb_4R_3–Sb_4R_3	Sb–Sb	2.823(3)–2.855(3)	134.5	$P2_1/c$	[22]
Ring A	Sb–C	2.21(3)–2.28(3)	134.9		
	Sb–Sb–Sb	84.84(8)–86.21(8)			
$Sb_4R_3Sb_4R_3$	Sb–Sb	2.845(3)–2.873(3)	135.5		
Ring B	Sb–C	2.21(3)–2.28(3)	137		
	Sb–Sb–Sb	83.45(8)–87.76(8)			

$(Me_3SiCH_2Sb)_5$ by X-ray diffraction failed owing to disorder phenomena. However, the structure of a complex with the pentastibolane ligand, $(Me_3SiCH_2Sb)_5[(W(CO)_5]_2$ was determined [28]. Recently, also the neopentylantimony ring system was investigated. As expected, the neopentyl and trimethylsilylmethyl antimony ring systems are closely related with preference for the pentamer in equilibria with the tetramer. A recent achievement is the first crystal structure determination of a pentastibolane [29]. The molecular structure of this antimony five ring is depicted in Fig. 2. The crystals consist of *cyclo*-$(Me_3CCH_2Sb)_5$ molecules in a distorted *envelope* conformation where four antimony atoms lie almost in a plane (mean deviation: 0.1690 Å) and the fifth antimony atom is 1.5291 Å above this plane. Through intermolecular Sb···Sb contacts of 4.2208 Å, which are close to the sum of the van der Waals radii of two antimony atoms (4.4 Å), there is a zig-zag chain association of the stibolane molecules. These weak intermolecular contacts may be responsible for the avoidance of disorder phenomena. Structural data of *cyclo*-R_5Sb_5 and related phosphorus and arsenic five rings are given in Table 2.

A general method for the synthesis of tetramers and pentamers is the dehalogenation of $RSbX_2$ (X = Cl, Br) with Mg. However, reduction with Cp_2Co or electrochemical methods were also used. Six-membered rings, *cyclo*-R_6Sb_6 exist with phenyl and tolyl substituents. They are stable only in the solid state. In solution, the ring size is not preserved but pentamers and tetramers form [2]. Solvates of the hexamers form by reaction of $PhSbH_2$ with styrene or by exposure of $PhSb(SiMe_3)_2$ to air [4]. Little is known of larger antimony rings. It is however likely that the black solid forms of ethyl- or propylantimony consist of large rings, $(RSb)_x$ (R = Et, Pr; $x \gg 6$) [17]. The ring size and the structures of these species, which in organic solvents are transformed in *cyclo*-pentamers or tetramers, are unknown.

Recently, also organo bismuth monocycles were prepared. Examples are $(RBi)_n$, $R = (Me_3Si)_2CH$, $n = 3, 4$ [34]; $R = Me_3SiCH_2$ [35], Me_3CCH_2 [29], $n = 3, 5$; $R =$ 2-$(Me_2NCH_2)C_6H_4Bi$, $n = 3, 4$ [36]; $R = (Me_3Si)_3Si$, $n = 4$ [37]. Methods for the synthesis of cyclobismuthines include dehalogenation of $RBiCl_2$ with Mg in thf, elimination of H_2 from $RBiH_2$, reaction of RLi with $BiCl_3$, and elimination of RH from R_2BiH. A common feature of the majority of bismuth ring systems is the preference for trimers in solution in ring–ring equilibria with tetramers ($R = (Me_3Si)_2CH$ [34], 2-$(Me_2NCH_2)C_6H_4$ [36]) or pentamers ($R = Me_3SiCH_2$ [35], Me_3CCH_2 [29]). *cyclo*-R_4Bi_4 [$R = (Me_3Si)_3Si$] [37] is exceptional because it does

Table 2
Geometric parameters of five-membered pnicogen rings

Compound	Molecular data (Å; °)		Conformation	Space group	References
$(CF_3P)_5$	P–P	2.202(7)–2.252(7)	Envelope	$P2_1/n$	[30]
	P–C	1.873(26)–1.925(22)			
	P–P–P	94.6(3)–107.5(3)			
$(PhP)_5$	P–P	2.207(5)–2.223(5)	Envelope	$P2_1/n$	[31]
	P–C	1.828(12)–1.858(13)			
	P–P–P	94.05(18)–107.24(19)			
$(MeAs)_5$	As–As	2.419–2.441	Twist	$P2_1/n$	[32]
	As–C	1.929–1.981			
	As–As–As	97.52–105.62			
$(Me_3SiCH_2As)_5$	As–As	2.424(1)–2.446(1)	Envelope	$P2_1/c$	[33]
	As–C	1.978(8)–2.014(7)			
	As–As–As	96.46(4)–105.24(4)			
$(Me_3CCH_2Sb)_5$	Sb–Sb	2.812(3)–2.820(3)	Envelope	$Pna2(1)$	[28]
	Sb–C	2.15(4)–2.28(3)			
	Sb–Sb–Sb	95.93(8)–103.85(8)			

not take part in ring–ring eqilibria. Only four-membered bismuth monocycles, $(RBi)_4$, R = $(Me_3Si)_2CH$ [34], 2-$(Me_2NCH_2)C_6H_4$ [36], $(Me_3Si)_3Si$ [37] were fully characterized by X-ray diffraction. Structures of two bismuth rings are shown in Fig. 4.

$(RBi)_4$, R = 2-$(Me_2NCH_2)C_6H_4$ [36] is a folded tetrabismetane with the 2-$(Me_2NCH_2)C_6H_4$ substituents in the *all-trans*-configuration. The Bi_3–Bi_3 dihedral angles are 107.9 and 109.4°, respectively. The orientation of the aryl groups leads to a propeller-like arrangement. The geometry about the bismuth atoms is distorted *pseudo*-trigonal bipyramidal with one of the neighbouring bismuth atoms and the nitrogen atom in axial positions [Bi–Bi–N 158.7(6)–163.5(5)°]; the second bismuth, the *ipso* carbon atom and the lone pair of electrons are in equatorial positions. The Bi–Bi–Bi angles [76.79(4)–79.51(4)°] are comparable with those found in *cyclo*-$[(Me_3Si)_2CH]_4Bi_4$ [78.97(8)–79.93(6)°] [1,34].

Sterical protection by bulky silyl substituents [R = $(Me_3Si)_3Si$ [37], $(Me_3C)_3Si$ [38]] leads to remarkably stable bismuth rings of the type *cyclo*-R_4Bi_4. Crystals consist of folded four rings with the substituents in the *all-trans*-configuration. Structural data of bismuth rings are given in Table 3.

4. Comparison of heavier pnicogen oligomers $(RE)_n$ (E = P, As, Sb, Bi; $n = 2$–6)

The comparison of oligomers of all the heavier pnicogens reveals several interesting trends. *trans*-Dimers are known for all the pnicogen elements, and it is not surprising that for the heaviest elements extremely bulky substituents are required. Cyclic oligomers $(RE)_n$ have been synthesized for P, As, Sb with $n = 3$–6 and for Bi with $n = 3$–5. Evidence for hexabismanes is still missing. The tendency to participate in ring–ring reactions with transformation of the ring size is increasing from phosphorus to bismuth rings. This trend corresponds to the decrease of single bond energies in the series: P–P 201 kJ/mol, As–As 146 kJ/mol, Sb–Sb 121 kJ/mol [39], and Bi–Bi 105 kJ/mol [40]. Transformations between cyclophosphines or cycloarsines occur only at elevated temperatures, whereas cyclostibines and cyclobismuthines readily take part in ring equilibria at or below room temperature if they are not sterically protected by bulky substituents [41]. The steric requirements for the protection of the rings with respect to ring–ring reactions increase with the size of the element. $(Me_3Si)_2CH$ groups suffice for the protection of Sb_4 rings but not for kinetically stable Bi_4 rings. For the protection of the latter, four $(Me_3Si)_3Si$ groups are required. All

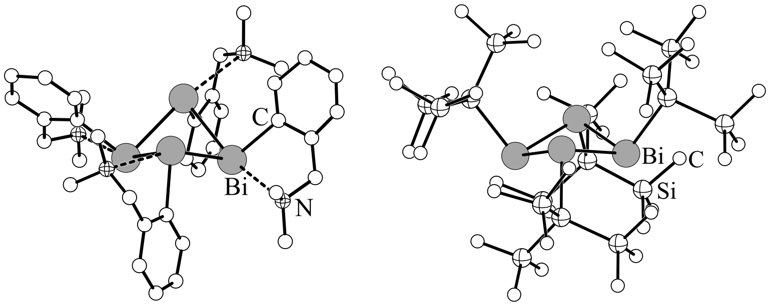

Fig. 4. Structures of tetrabismetanes R_4Bi_4 (R = 2-(dimethylaminomethyl)phenyl) [36], R = $(Me_3Si)_3Si$ [37].

Table 3
Geometric parameters of bismuth homocycles

Compound	Molecular data (Å; °)		Fold angles (°)	Space group	References
$[(Me_3Si)_2CHBi]_4$	Bi–Bi	2.970(5)–3.023(2)	112.6	$P\bar{1}$	[1,34]
	Bi–C	2.32(2)–2.390(19)	112.9		
	Bi–Bi–Bi	78.97(8)–79.93(6)			
$[2\text{-}(Me_2NCH_2)C_6H_4Bi]_4$	Bi–Bi	3.009(2)–3.0221(2)	107.9	$P2(1)2(1)2(1)$	[36]
	Bi–C	2.24(3)–2.30(3)	109.4		
	Bi–Bi–Bi	76.79(4)–79.51(4)			
$[(Me_3Si)_3SiBi]_4$	Bi–Bi	3.013(6)–3.0302(5)	138	$P2_1/n$	[37]
	Bi–Si	2.694(3)–2.726(3)			
	Bi–Bi–Bi	84.65(1)–87.41(1)			
$[(Me_3C)_3SiBi]_4$	Bi–Bi	3.013(1)–3.038(2)	150	$C2/c$	[38]
	Bi–Si	2.750(6)–2.765(5)			
	Bi–Bi–Bi	87.97(2)–88.10(2)			
$[(Me_3Si)_3Sn)]_6Bi_8$	Bi–Bi	2.972(2)–3.019(2)	115	$P2_1/n$	[37]
	Bi–Sn	2.897(3)–2.961(3)	115.8		
	Bi–Bi–Bi	89.37(6)–105.28(6)			

the bismuth four and five rings with less steric protection are transformed in solution into trimers when the temperature is increased and the concentration is decreased. Apparently a three-membered organobismuth ring is not under very large strain, although deformation of the bond angles in the ring to 60°, eclipsed conformations of the Bi–Bi bond and of two Bi–C bonds as well as repulsion between the substituents in *cis*-positions should disfavor this ring size.

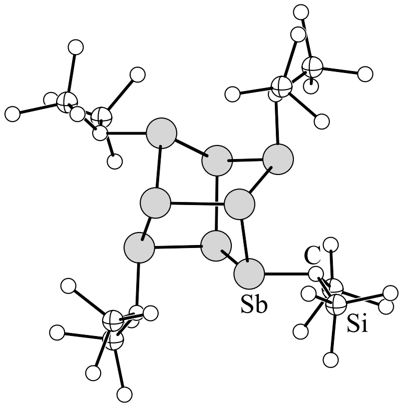

Fig. 5. Structure of R_4Sb_8 in $R_4Sb_8{\cdot}thf$, R = $(Me_3Si)_2CH$ [22].

5. Polycyclic stibines and bismuthines, R_nE_m ($n < m$)

Three polycyclic stibines, namely R_5Sb_7, R_4Sb_8 and R_6Sb_8 [R = $(Me_3Si)_2CH$] are known. R_5Sb_7 and R_4Sb_8 are formed in low yield as side products of the dehalogenation of $RSbCl_2$ with Mg in thf [1]. A more efficient method, giving R_4Sb_8 in 32% yield, is the reaction of $RSbH_2$ with $SbCl_3$ in presence of pyridine. Both the unsolvated form of R_4Sb_8 and the solvate $R_4Sb_8{\cdot}thf$ were characterized by X-ray diffraction [22]. The polycyclic molecules in both forms are similar, the latter being more symmetrical. They consist of five-membered antimony rings and can be derived from a tetrahedral Sb_4 unit, where four opposite edges are bridged by RSb groups. In the solvated form, there are stacks of polycycles surrounded by disordered thf molecules. The molecular structure of R_4Sb_8 in the thf solvate is depicted in Fig. 5.

NMR spectra in benzene show that all of the substituents are equivalent in solution. R_4Sb_8 is sensitive to light. The photochemical reaction leads to *cyclo*-R_3Sb_3. R_5Sb_7 was characterized only by mass spectrometry. The structural features are unknown, but a bicyclic norbornane type structure [1] is probable. The polycycle R_6Sb_8 was reported only very recently [22]. It formed as a rearrangement product in an attempt to metallate $R_2Sb_2H_2$ with ${}^tBuONa$ in presence of 18-crown-6. The structure corresponds to a known motif in pnicogen chemistry. Two-folded four-membered rings with *all-trans* substituents are connected through a Sb–Sb bond. The structure is depicted in Fig. 6. The deviation from the ideal trans conformation results from the packing of the $(Me_3Si)_2CH$ substituents. The conformation along the Sb(4)–Sb(5) bond is intermediate between anticlinal and

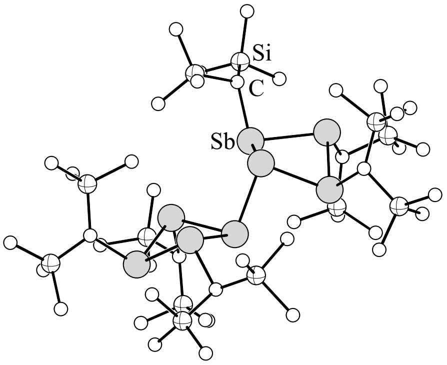

Fig. 6. Structure of R_6Sb_8, R = $(Me_3Si)_2CH$ [22].

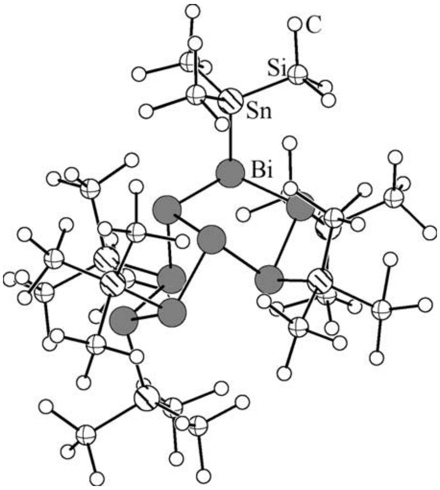

Fig. 7. Structure of $Bi_8(SnR_3)_6$ ($R = SiMe_3$) [37].

antiperiplanar with dihedral angles lp–Sb(4)–Sb(5)–lp = 135.19(1)° (lp = assumed direction of the lone pairs of electrons at the Sb atoms).

The first polycyclic bismuthine was reported by Linti and Köstler [37]. Reaction of $R_3SnLi(thf)_3$ with $BiBr_3$ gave $Bi_8(SnR_3)_6$ ($R = SiMe_3$) (Eq. (3)). The structure of this polycycle consists of a bicyclo(3.3.0) octane like core (Fig. 7). There are two folded five rings connected through a Bi–Bi bond. The substituents are in *trans* positions. The Bi–Bi bond lengths (2.972–3.019 Å) and the Bi–Bi–Bi angles (89.37–105.28°) are comparable with those found in $[(Me_3Si)_3Si]_4Bi_4$ (Bi–Bi 3.0134(6)–3.0302(5) Å, Bi–Bi–Bi 84.65(1)–87.41(1)°).

$$R_3SnLi(thf)_3 \xrightarrow[-LiBr,\,-(R_3Sn)_2]{+BiBr_3} Bi_8(SnR_3)_6, \quad R = SiMe_3 \tag{3}$$

6. Distibines and dibismuthines, R_4E_2

The chemistry of distibines and dibismuthines have received attention because some examples show unusual color phenomena related to linear antimony or bismuth chains formed by the association of the molecules in the solid state. Several reviews have been published in this field [2,5,42]. Recently, a distibine with two hydrogen atoms as substituents, R(H)SbSb(H)R [$R = (Me_3Si)_2CH$] was synthesized and characterized by various methods including X-ray diffraction [43], neutron diffraction [22], and NMR spectroscopy. The distibine is formed by addition of $LiAlH_4$ to $RSbCl_2$ in diethylether probably through elimination of HCl from the intermediates RSb(H)Cl and $RSbH_2$ (Eq. (4)).

$$RSbCl_2 \xrightarrow{LiAlH_4} RSb(H)Cl \xrightarrow[-HCl]{RSbH_2} R(H)Sb\text{–}Sb(H)R, \quad R = (Me_3Si)_2CH \tag{4}$$

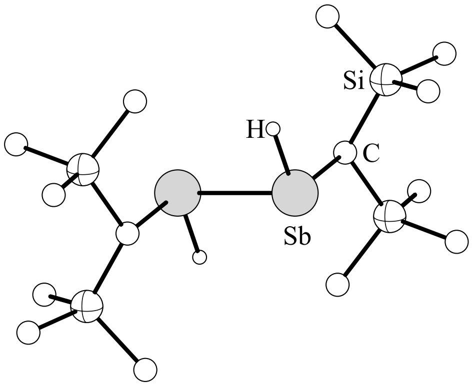

Fig. 8. Structure of *meso*-R(H)SbSb(H)R, $R = (Me_3Si)_2CH$ [22,43].

R(H)SbSb(H)R [$R = (Me_3Si)_2CH$] exists in the solid state as *meso*-isomer in the antiperiplanar conformation (Fig. 8) with an Sb–Sb bond length of 2.8304 Å. Similar values were found in Me_4Sb_2 (Sb–Sb 2.84 Å, [44] 2.86 Å [45]) and Ph_4Sb_2 (Sb–Sb 2.834 Å [46]).

In the solid state, the molecules are associated to zig-zag chains through weak Sb···Sb contacts (4.2 Å). The Sb–H bond length determined by neutron diffraction is 1.705(1) Å. The signals for the Sb–H valence vibration appears at 1849 cm^{-1} in the infrared and at 1839 cm^{-1} in the Raman spectrum. The ^1H NMR spectrum shows that *meso*-R(H)SbSb(H)R is partially transformed in C_6D_6 into an equilibrium mixture of $RSbH_2$, $R(H)Sb(SbR)_nSb(H)R$ ($n = 1, 2$) and *d,l*-R(H)SbSb(H)R (Eq. (5)). Aged solutions also contain signals of R_3Sb_3 and the reaction of R_3Sb_3 with $RSbH_2$ gives back R(H)SbSb(H)R. The deuterium analogues were prepared by the reaction of $RSbCl_2$ with $LiAlD_4$. The ^2H spectrum of a solution of R(D)SbSb(D)R in C_6H_6 is shown in Fig. 9. The spectrum

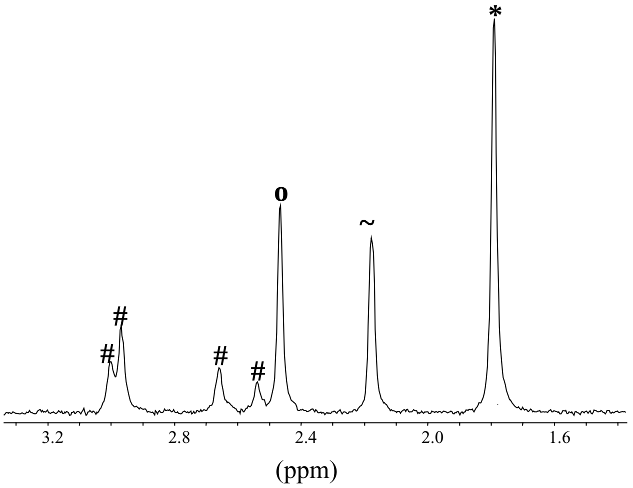

Fig. 9. ^2H NMR spectrum (81.92 MHz) of R(D)Sb–Sb(D)R [$R = (Me_3Si)_2CH$] in C_6D_6 at room temperature. (∗) *d,l*-R(D)Sb–Sb(D)R; (0) *meso*-R(D)Sb–Sb(D)R; (∼) $RSbD_2$; (#) $R(D)Sb(SbR)_nSb(D)R$ ($n = 2, 3$); $R = (Me_3Si)_2CH$.

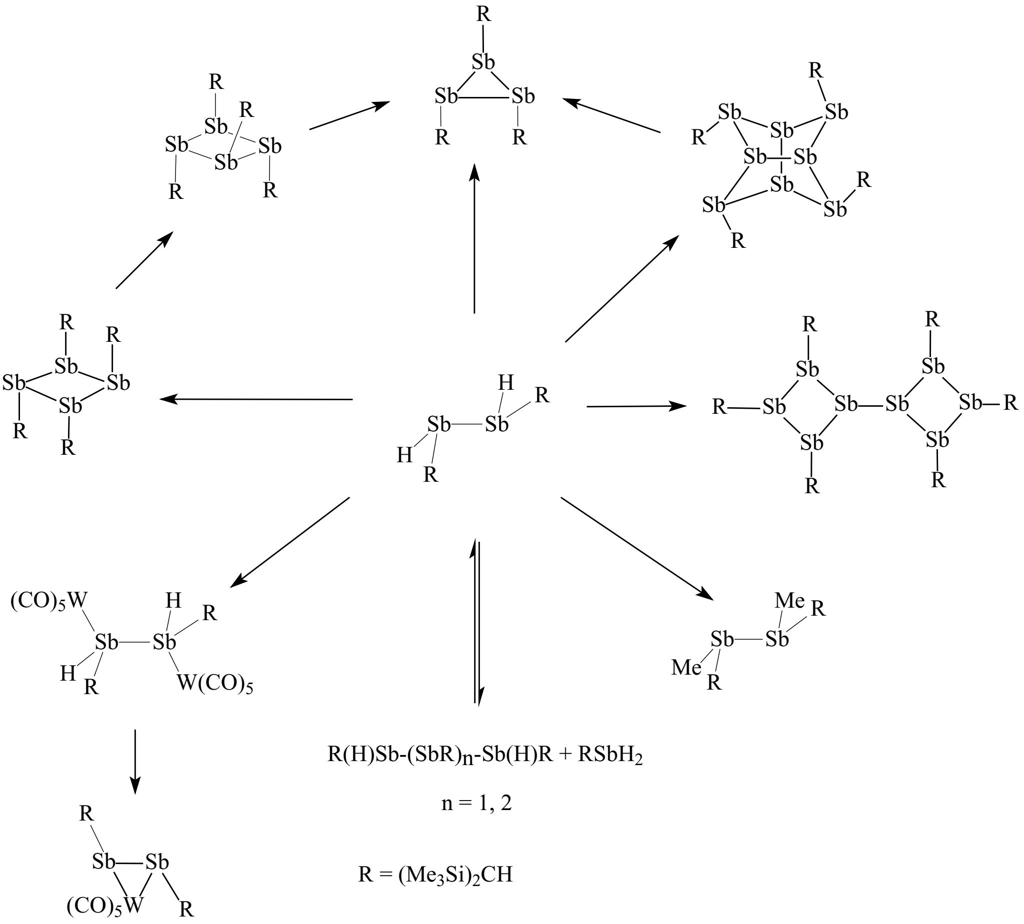

Scheme 2.

contains signals of *meso*-, *d,l*-R(D)SbSb(D)R, $RSbD_2$, and $R(D)Sb(SbR)_nSb(D)R$ ($n = 1, 2$).

$$\begin{tikzcd}
2\,meso\text{-}R(H)SbSb(H)R \arrow[r, rightleftharpoons] \arrow[d, shift left] & 2\,d,l\text{-}R(H)SbSb(H)R \\
RSbH_2 + R(H)Sb\text{-}SbR\text{-}Sb(H)R \arrow[u, shift left] \arrow[r, rightleftharpoons] & 2/3\, R_3Sb_3 + RSbH_2
\end{tikzcd}$$

$R = (Me_3Si)_2CH$

(5)

Complexation with transition metal carbonyl fragments inhibits the equilibration and *meso*- and *d,l*-derivatives can be separated. Substitution of the hydrogen atoms by methyl groups occurs by reaction of CH_3I in presence of DBU, and *meso*- and *d,l*-forms of $R(CH_3)SbSb(CH_3)R$ as well as $RSb(H)CH_3$ are obtained.

R(H)SbSb(H)R [$R = (Me_3Si)_2CH$] or more precisely the equilibrium mixture obtained by dissolving *meso*-R(H)SbSb(H)R in organic solvents proved to be a valuable starting material for a wide variety of known and novel bis(trimethylsilyl)methyl antimony compounds. An overview is given in Scheme 2.

A dibismuthine bearing four bis(trimethylsilyl)methyl groups is formed by hydrogen elimination from R_2BiH [$R = (Me_3Si)_2CH$] [47]. The solid state structure consists of R_2BiBiR_2 molecules in a near antiperiplanar (*trans*) conformation. The NMR spectra in C_6D_6 or $C_6D_5CD_3$ show characteristic changes with variation of the concentration or the temperature. Intact molecules are observed only at very low concentration (7×10^{-7} M). Spectral changes at higher concentration and lower temperature correspond to the exchange of R_2Bi groups with inversion of configuration through dimeric association (Eq. (6)).

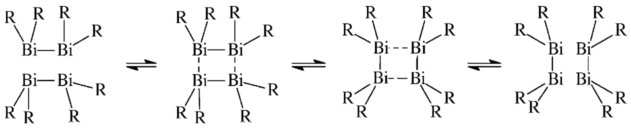

$R = (Me_3Si)_2CH$

(6)

The crystal structure of R_2BiBiR_2 [$R = (Me_3Si)_2CH$] consists of molecules in the *trans* conformation with an dihedral angle, lp–Bi–Bi–lp of 164.23° (lp denotes the direction of the lone pair of electrons at Bi, derived from crystallographic data looking for empty spaces). The Bi–Bi bond length of 3.0534 Å, corresponds to a normal bismuth–bismuth single bond.

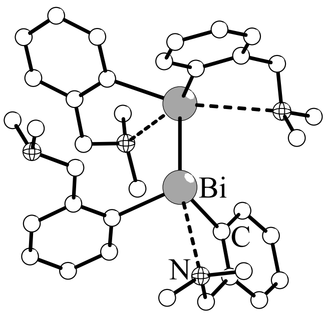

Fig. 10. Structure of R_4Bi_2 (R = 2-(dimethylaminomethyl)phenyl) [36] in the crystal.

A dibismuthine R_2BiBiR_2 with $R = 2\text{-}(Me_2NCH_2)C_6H_4$ was synthesized by reduction of R_2BiCl with Mg in THF at −40 °C (Eq. (7)) [36]. The crystal structure (Fig. 10) consists of dibismuthine molecules in the near antiperiplanar (*trans*) conformation as well [lp–Bi–Bi–lp 132.18(1) and 35.2(2)°]. Intramolecular N–Bi coordination occurs only through three of the four nitrogen atoms. This coordination pattern results in a wide range of Bi–Bi–C angles [81.77(14)–106.33(14)°] and different overall coordination geometries at the metal atoms. One of the bismuth atoms is in a distorted *pseudo*-trigonal bipyramidal environment. The coordination geometry around the other bismuth atom is distorted tetragonal pyramidal. The Bi–Bi distance is 3.0657(5) Å.

$$2R_2BiCl + Mg \xrightarrow[-40\,^\circ C]{thf} R_2Bi\text{–}BiR_2 + MgCl_2, \quad R = 2\text{-}(Me_2NCH_2)C_6H_4 \qquad (7)$$

7. Catenastibines and bismuthines, $R_{(n+2)}E_n$ (E = Sb, Bi; $n = 3, 4$)

Catenastibines form when cyclostibines react with distibines in ring chain equilibria [2]. In absence of bulky terminal groups, they exist in solution only in presence of excess distibine or cyclostibines because the decomposition of catenastibines according to Eq. (8) is favored by entropy.

$$R_2Sb\text{–}SbR_2 + cyclo\text{-}(RSb)_n \rightleftharpoons R_2Sb\text{–}(RSb)_n\text{–}SbR_2, \quad R = \text{Alkyl, Aryl} \qquad (8)$$

The tetrastibines formed in this equilibrium were trapped as ligands in $Cr(CO)_4$ complexes. For the tetrastibines which bear two identical groups on the central Sb atoms three isomers (the *meso*- and *d,l*-forms) are possible. Only the *d,l*-forms are trapped as ligands. The first achievements including X-ray crystallography in this field were already reviewed [8]. Recently, a complex containing a catena-tetrastibine ligand with different substituents on the central antimony center was obtained. An X-ray diffraction study revealed that only two of the four possible isomers, the enantiomers of the *threo* form are present in crystals of *cyclo*-[$Cr(CO)_4(Ph_2Sb\text{–}SbPh\text{–}SbR\text{–}SbPh_2)$]; R = Me_3SiCH_2 [48]. The structure (Fig. 11) features a five-membered chelate ring where the Sb(2)–Sb(3) unit is twisted by 23° out of the Sb(1)–Cr–Sb(4) plane. A remarkable feature of the crystal structure of *cyclo*-[$Cr(CO)_4(Ph_2Sb\text{–}SbPh\text{–}SbR\text{–}SbPh_2)$], R = Me_3SiCH_2 is the pair wise association of two enantiomers through a short intermolecular contact (3.636 Å) between two antimony atoms bearing phenyl groups.

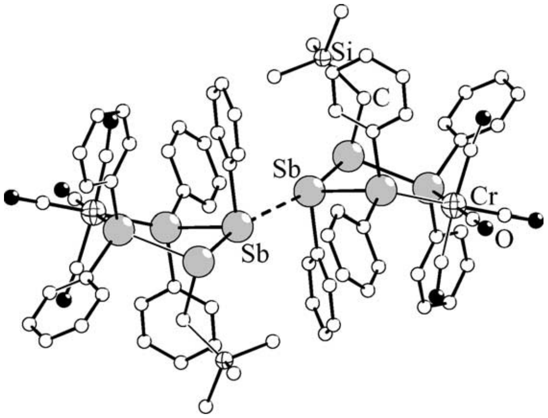

Fig. 11. Structure of *cyclo*-[$Cr(CO)_4(Ph_2Sb\text{–}SbPh\text{–}SbR\text{–}SbPh_2)$] R = Me_3SiCH_2 [48].

Catenastibines (e.g., $Ph_2Sb\text{–}SbPh\text{–}SbPh_2$, $Me_2Sb(SbMe)_{11}SbMe_2$) exist in the absence of other components as solid materials, which are insoluble or unstable in solution. Attempts to determine the structures of these materials were unsuccessful. Recently, the first tri- and tetrastibines, which are stable in solution, were described. Following the idea that catenastibines can be stabilized by bulky substituents which protect the chain molecules both kinetically, because they hinder intermolecular Sb · · · Sb contacts, and thermodynamically, because bulky terminal groups disfavor the distibines, the synthesis of ${}^tBu_2Sb(SbMe)_nSb{}^tBu_2$ [$n = 1, 2$] and $Mes_2Sb(SbPh)_nSbMes_2$ [$n = 1, 2$] was carried out by reactions (9) and (10) [49].

$$R_2SbCl \xrightarrow[-MgCl_2]{+CH_3SbCl_2+Mg/thf,\ 25\,^\circ C} R_2Sb(SbCH_3)_nSbR_2, \quad R = {}^tBu \text{ and } n = 1, 2 \qquad (9)$$

$$Mes_2SbLi \xrightarrow[-LiCl]{+PhSbCl_2/thf,\,-70\,^\circ C} Mes_2Sb(SbPh)_nSbMes_2, \quad n = 1, 2 \qquad (10)$$

The novel tri- and tetrastibines were characterized by NMR spectroscopy taking advantage of the characteristic NMR patterns which result from the diastereotopic situation of the terminal organo substituents. A spectrum of a solution of ${}^tBu_2Sb(SbMe)_nSb{}^tBu_2$ [$n = 1, 2$] is shown in Fig. 12.

The separation of the tristibines from the tetrastibines was however not achieved mainly because the antimony chain

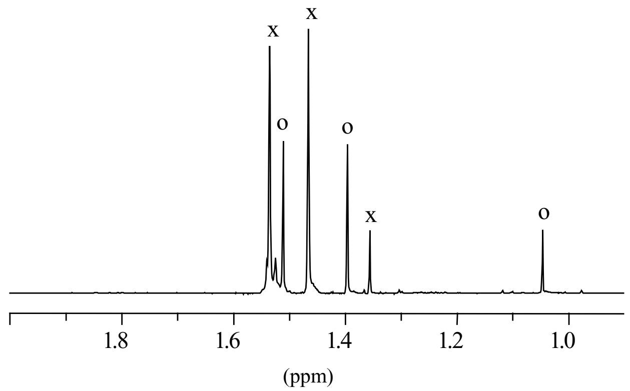

Fig. 12. ^{1}H NMR spectrum of a C_6D_6 solution containing *catena*-^{t}Bu$_2$Sb–SbCH$_3$–Sb^{t}Bu$_2$ (×), and *catena*-^{t}Bu$_2$Sb(SbCH$_3$)$_2$Sb^{t}Bu$_2$ (o).

compounds decompose readily with migration of the organo groups.

8. Adducts, cations and anions with Sb–Sb bonds

Dative Sb–Sb bonds occur in crystalline adducts between Me_3Sb and SbI_3 or $MeSbI_2$ of the type $[Me_3Sb–SbI_3{\cdot}thf]_2$ or $[Me_3Sb–Sb(Me)I_2]_2$ [2]. Addition of Me_4Sb_2 to Me_2SbBr leads to an ionic crystalline compound, i.e. $[Me_2Sb–SbMe_2–SbMe_2][Me_2SbBr_2]$. The cation of the latter compound can be viewed as a tetramethyldistibine adduct of the dimethylstibenium ion, Me_2Sb^+. More recently, also a trimethylstibine adduct of Me_2Sb^+ was reported as the cation of $[Me_3Sb–SbMe_2][MeSbBr_3]_2$. The compound was formed by a scrambling reaction starting from Me_2SbBr [50]. Another way to view $[Me_3Sb–SbMe_2]^+$ is to consider it as a product of formal addition of Me^+ to $Me_2SbSbMe_2$. A product of the formal addition of two Me^+ ions to Me_4Sb_2 is also known. The resulting dication $[Me_3Sb–SbMe_3]^{2+}$ was obtained as an $SbF_6{}^-$ salt by hydrogen elimination from $[Me_3SbH]^+[SbF_6]^-$ [51]. The molecular formulae of $Me_2SbSbMe_2$, $Me_3SbSbMe_2{}^+$ and $Me_3SbSbMe_3{}^{2+}$ are given in Scheme 3.

It is remarkable that the Sb–Sb bond lengths, $Me_2SbSbMe_2$ (2.836(1) Å), $Me_3SbSbMe_2{}^+$ 2.8205(12) and $Me_3SbSbMe_3{}^{2+}$ (2.7624(11), 2.7867(12) Å) decrease with addition of methyl groups. The inspection of the bond angles at antimony supports the assumption of almost pure p-orbitals involved in bonding in $Me_2SbSbMe_2$, sp^3- and p-orbitals in $Me_3SbSbMe_2{}^+$, and sp^3–sp^3 in $Me_3SbSbMe_3{}^{2+}$. Increasing s orbital participation leads to shorter bonds. However, the bond lengths may also be influenced by intermolecular contacts. Distances and angles of the cations are given in Table 4.

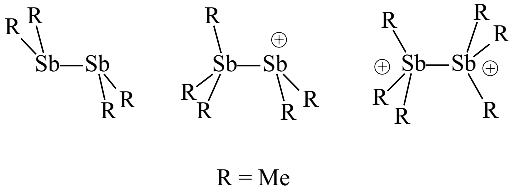

Scheme 3.

Known organometallic anions with Sb–Sb bonds include two triantimonides $[R_2Sb–Sb–SbR_2]^-$ (R = Ph, ^{t}Bu) [1,2]. Recently, also a diantimonide was described and the coordination of $[R_2SbSbR]^-$ and $[R_2Sb–Sb–SbR_2]^-$ (R = ^{t}Bu) was studied [52]. The ^{t}Bu antimony compounds are obtained by the reaction of ^{t}Bu$_4$Sb$_4$ with Na or K in thf and pentamethylethylenetriamine (pmedta) (Eq. (11)).

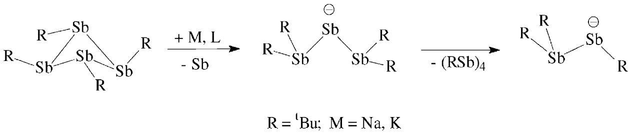

(11)

The type of coordination of $[R_2Sb–Sb–SbR_2]^-$ (R = ^{t}Bu) depends on the nature of the alkali metal and on the number of pmedta ligands coordinated on the alkali metal centers. When the K center is completely covered by two pmedta ligands there are no close interactions between the anion and the cation [1]. With a K/pmedta ratio of 1:1 there is coordination of the triantimonide on two neighboring potassium centers in a monodentate fashion through the central Sb atom and in a bidentate fashion through the terminal

Table 4
Geometric parameters of $Me_2SbSbMe_2$, $Me_3SbSbMe_2{}^+$ and $Me_3SbSbMe_3{}^{2+}$

Compound	Sb–Sb (Å)	Configuration	Angles (°)		References
$Me_2SbSbMe_2$	2.84, 2.86	p^3	C–Sb–Sb C–Sb–C	94.37(1), 94.89(1) 88.53–100.66	[2]
$Me_3SbSbMe_2{}^+$	2.8205(12)	sp^3, p^3	C–Sb–Sb C–Sb–C	91.0(4), 91.3(3) 94.3(5)–104.4(5)	[50]
$Me_3SbSbMe_3{}^{++}$	2.7624(11); 2.7867(12)	sp^3, sp^3	C–Sb–Sb C–Sb–C	104.88–110.87 107.63–115,41	[51]
$Me_2SbSbMe_2SbMe_2{}^+$	2.8203(4)	2 × p^3, 1 × sp^3	Sb–Sb–Sb C–Sb–C	116.19(2) 94.3(2)–98.0(4)	[2]

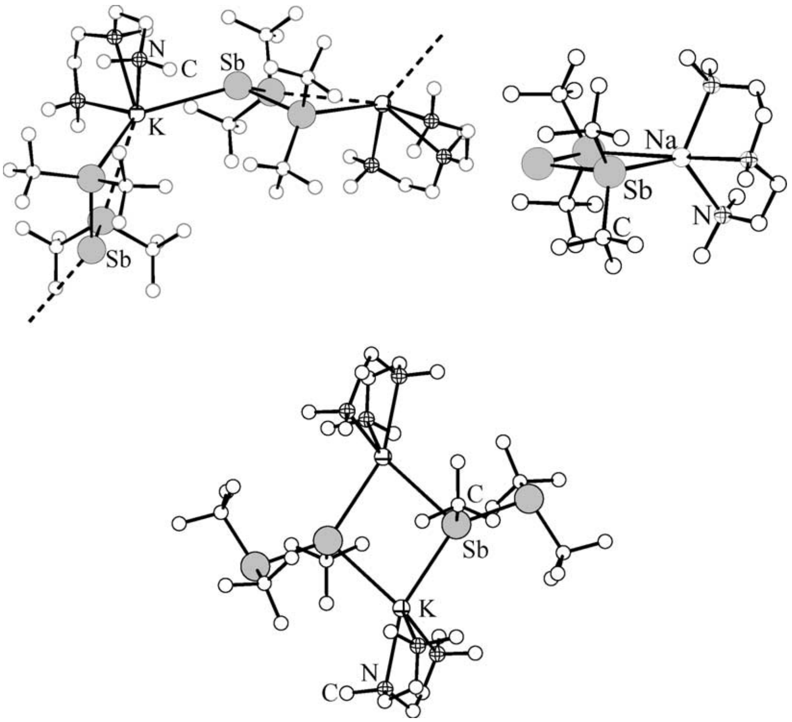

Fig. 13. Structures of $[M(L)({}^tBu_4Sb_3)]$ M = Na, K; $[K(L)({}^tBu_3Sb_2)]$, L = $[Me_2N(CH_2)_2]_2NMe$ (pmedta) [52].

antimony atoms. Also, the pmedta·K units are bridging and an extended chain structure results (Fig. 13).

Geometric parameters are listed in Table 5.

It is remarkable that both the cationic and the anionic di- and triantimony species have significantly shorter Sb–Sb bonds than the neutral distibines or cyclostibines. It is hard to believe that the lone pairs at antimony or (p–d)π bonding should be responsible for the shortening of the bonds in the ionic species. [53] We suggest that the explanation lies in the different types of hybridization. The geometric parameters of distibines and cyclostibines, i.e. bond angles close to 90°, correspond to the p^3 configuration with the lone pairs of electrons in an s-orbital. The geometry of the four coordinate cationic centers corresponds to the sp^3 configuration. The geometry around the anionic antimony centers in $K(L){}^tBu_4Sb_3$ approaches the requirements for sp^3 hybridization as well. In $K(L){}^tBu_3Sb_2$, the anionic Sb is in a trigonal planar environment of two K atoms and one Sb atom with the ${}^tBu$ group orientated perpendicular to the basal plane. This geometry corresponds to sp^2 hybridization for the Sb–Sb and Sb–K bonding and to the use of a p-orbital for the Sb–C bonds. These examples show that in all ionic examples the geometric parameters suggest hybridization with s orbital participation for the Sb–Sb bonds which is consistent with shorter bonds than the use of unhybridized orbitals.

9. Complexes with stibine, distibine, dibismuthine and catena–stibine ligands

Compounds with ligands or starting materials containing Sb–Sb or Bi–Bi bonds that have recently been under investigation are schematically depicted in Scheme 4.

Table 5
Geometric parameters of anions with Sb–Sb bonds in different environments

Compound	Sb–Sb (Å)	Angle (°)		Configuration	References
${}^tBu_4Sb_4$	2.814–2.821	Sb–Sb–Sb	84.8(1)–85.2(1)	4 × p^3	[23]
$K(L)_2{}^tBu_4Sb_3$	2.764, 2.7669	Sb–Sb–Sb	86.23(3)	2 × p^3, 1 × sp^2	[1]
$K(L){}^tBu_4Sb_3$	2.767(1), 2.763(3)	Sb–Sb–Sb	87.60(5)	2 × sp^3, 1 × sp^2	[52]
$Na(L){}^tBu_4Sb_3$	2.720(8)–2.776(2)	Sb–Sb–Sb	89.80(7)	2 × p^3, 1 × sp^2	[52]
$K(L){}^tBu_3Sb_2$	2.7613(10)	Sb–Sb–K	113.85(2), 143.67(18)	1 × p^3, 1 × sp^2	[52]
$LiL'_nPh_4Sb_3$	2.762(2)	Sb–Sb–Sb	88.79(1)	2 × p^3, 1 × sp^2	[2,53]
Ph_4Sb_2	2.837	C–Sb–C	94.36(1)	2 × p^3	[2]
		C–Sb–Sb	93.78(1), 96.50(1)		

L: pmedta; L′: [12-crown-4].

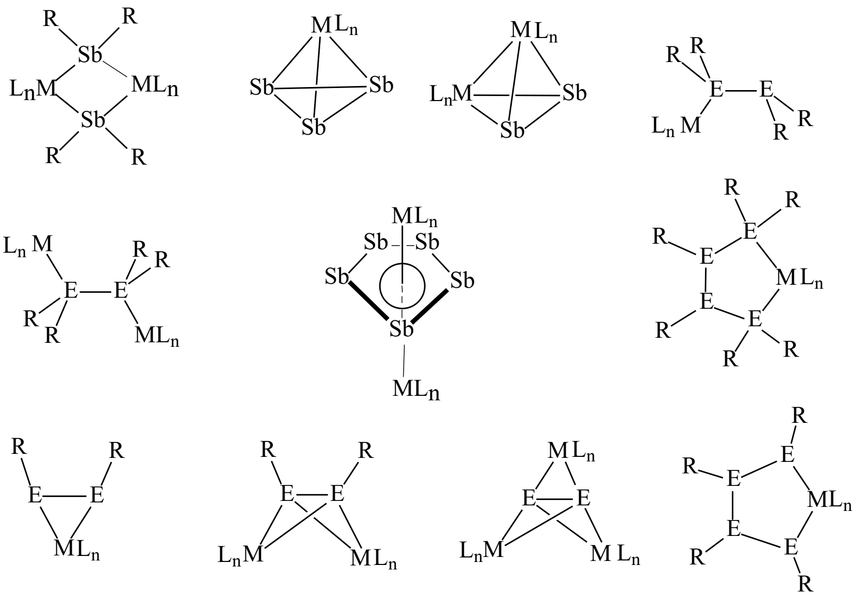

R = monovalent organic group; ML_n = transition metal complex fragment; E = Sb, Bi

Scheme 4.

Complexation reactions of tetraorganodistibines with transition metal carbonyl complexes give compounds of the types $(R_2Sb–SbR_2)ML_n$, $L_nM(R_2Sb–SbR_2)ML_n$ and $[L_nMSbR]_2$. Recently, the structure of $(CO)_5Cr(Me_2SbSbMe_2)Cr(CO)_5$, a complex with the tetramethyldistibine ligand, was determined. The structure is shown in Fig. 14. The coordination of the distibine leads to wider angles and shorter bonds at the antimony atoms $[Me_4Sb_2/(CO)_5Cr(Me_2SbSbMe_2)Cr(CO)_5]$, SbC_2, 92.2–95.2/99.2–100.34°; CSbSb, 94.27–94.65/96.94–102.6°; Sb–Sb, 2.84/2.809 Å. These changes in the geometry probably result from an increase of s-orbital participation from the p^3 configuration in Me_4Sb_2 to nearly sp^3 in the complex. An unusual feature of the structure is a substantial deviation (dihedral angle lp–Sb–Sb–lp = 160°, lp = lone pair of electrons at Sb) from the ideal antiperiplanaric (*trans*) conformation (lp–Sb–Sb–lp = 180°) which was found in solid Me_4Sb_2 [5] and $(CO)_5MPh_2SbSbPh_2M(CO)_5$ (M = Cr [2], W [2]).

Another recent development is the coordination chemistry developed from $RSbH_2$ and R(H)Sb–Sb(H)R, R = $(Me_3Si)_2CH$. Thus $RSbH_2$ reacts with $W(CO)_5$thf to give $H_2(R)SbW(CO)_5$ [22]. Upon elimination of H_2 this complex gives $RSb[W(CO)_5]_2$, a blue stibinidene complex that was previously prepared from $RSbCl_2$ and $Na_2W_2(CO)_{10}$ [54].

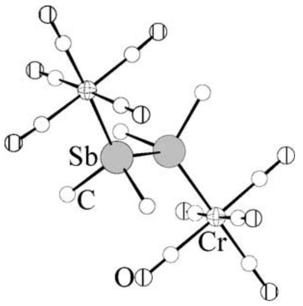

Fig. 14. Structure of $[Cr(CO)_5(Me_2Sb–SbMe_2)Cr(CO)_5]$ [45].

Reaction of R(H)Sb–Sb(H)R with $W(CO)_5$thf gives not only *meso*- but also *d,l*-$(CO)_5W[R(H)Sb–Sb(H)R]W(CO)_5$ [R = $(Me_3Si)_2CH$] by selective crystallization. The *meso*-form can be separated from the *d,l*-forms. In crystals of the *d,l*-forms both enantiomers are present in the 1:1 molar ratio. The structures are depicted in Fig. 15.

The Sb–Sb bond lengths 2.833 Å in *meso*- and 2.842 Å in *d,l*-$(CO)_5W[R(H)Sb–Sb(H)R]W(CO)_5$ [R = $(Me_3Si)_2CH$] lie in the normal range for a single bond. The *meso*-isomer adopts a conformation between antiperiplanar (*trans*) and anticlinal with the dihedral angles C–Sb–Sb–C 157.8(4)°, W–Sb–Sb–W 160.30(4)°, and H–Sb–Sb–H 157.31(1)°. The conformation of the *d,l*-isomers is close to *syn* with almost eclipsed positions of the $W(CO)_5$ groups and the hydrogen atoms with respect to the alkyl groups. The dihedral angles in the *d,l*-isomer are W–Sb–Sb–W 23.74(1), H–Sb–Sb–C 0.95(1), C–Sb–Sb–C 87.7(1)°. The environment of the antimony centers is distorted tetrahedral.

Reaction of $RSbH_2$ with $W(CO)_5$thf in the dark gives $RH_2SbW(CO)_5$ in good yield [22] (Eq. (12)). Elimination of hydrogen from $RH_2SbW(CO)_5$ leads to a *trans*-RSb=SbR$(W(CO)_5$, R = $[(Me_3Si)_2CH]$ [22] and $RSb[W(CO)_5]_2$ [54].

$$RSbH_2 + W(CO)_5\text{thf} \xrightarrow[-\text{thf}]{} R(H)_2SbW(CO)_5, \quad R = (Me_3Si)_2CH \qquad (12)$$

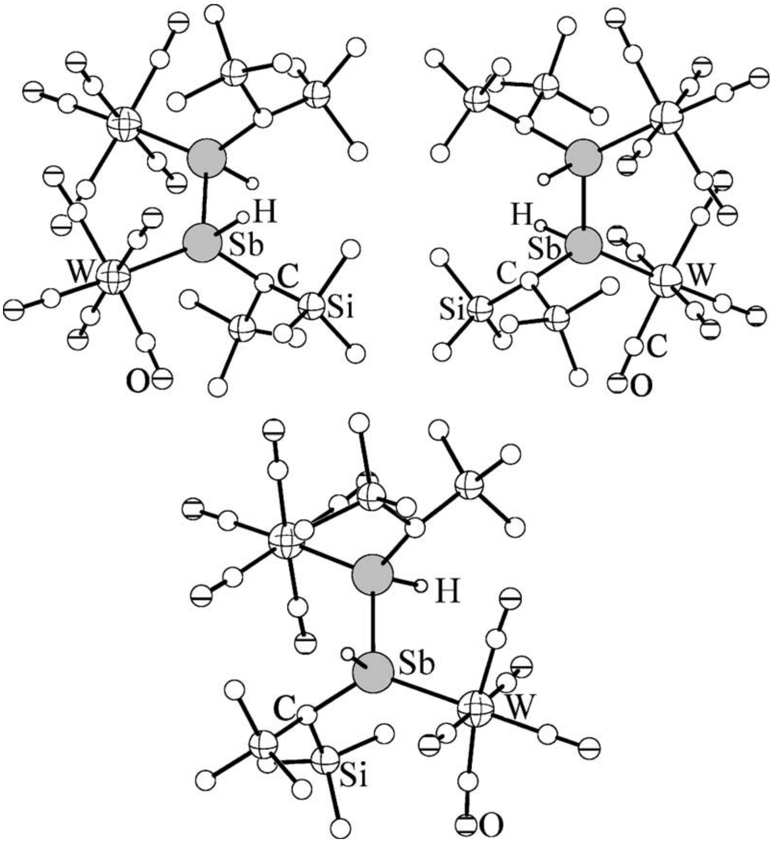

Fig. 15. Structures of the isomers of $(OC)_5W[R(H)Sb–Sb(H)R]W(CO)_5$ R = $(Me_3Si)_2CH$ [22].

Solutions of *meso*- and *d,l*-$(CO)_5W[R(H)Sb–Sb(H)R]W(CO)_5$ [R = $(Me_3Si)_2CH$] are stable only for a short time. NMR studies show that at room temperature after several hours isomerization between the *meso*- and *d,l*-forms occurs and signals of RSb=SbRW$(CO)_5$, [R = $(Me_3Si)_2CH$] [22] emerge. Quantitative transformation is achieved at 105 °C in C_6D_6 within 1 h (Scheme 2). RSb=SbRW$(CO)_5$, [R = $(Me_3Si)_2CH$] was characterized by single crystal structure analysis. The structure is depicted in Fig. 16. It is a *trans* distibene *side-on* coordinated to the W$(CO)_5$ fragment. The Sb–Sb bond length, 2.7413 Å is comparable with the corresponding values in distibene complexes with *side-on* ($R_2Sb_2Fe(CO)_4$ R = $(Me_3Si)_2CH$ 2.774 Å [55]), or *side-on*/*end-on* ($Ph_2Sb_2[W(CO)_5]_3$, 2.706 Å) coordination [56]. The Sb–W distances 2.991, 2.949 Å, are longer than the sum of the covalent radii of Sb and W (2.78 Å), and slightly longer than those found in the *meso*- or *d,l*-forms of $(CO)_5W[R(H)Sb–Sb(H)R]W(CO)_5$ (2.7755–2.792 Å) [22]. Geometric parameters of distibine and distibene complexes are summarized in Table 6.

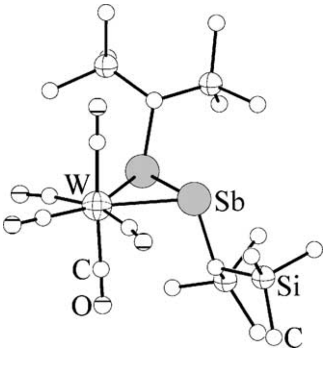

Fig. 16. Structure of *trans*-[RSb=SbR]W$(CO)_5$ R = $(Me_3Si)_2CH$ [22].

10. Reactions of cyclostibines and cyclobismuthines with transition metal carbonyl derivatives

Cyclostibines react with transition metal carbonyl complexes in various ways. The most straight forward type of reaction is the coordination of intact rings [^{t}Bu$_4$Sb$_4$, $(Me_3SiCH_2Sb)_5$, $[(Me_3Si)_2CHSb]_3$] to 16 electron transition metal carbonyl fragments. Both, 1:1 and 1:2 complexes were obtained [1] with W$(CO)_5$thf or $Fe_2(CO)_9$ as precursors. Recent examples of complexes with cyclostibine ligands are $(Me_3SiCH_2Sb)_5[W(CO)_5]_2$ and $[(Me_3Si)_2CHSb]_3W(CO)_5$. The structures of these complexes are depicted in Fig. 17.

The five ring in $(Me_3SiCH_2Sb)_5[W(CO)_5]_2$ [28] has an envelope conformation. Three trimethylsilylmethyl groups are in *trans* and two are in *cis* positions. The W$(CO)_5$ groups occupy 1,3 positions, *trans* to each other.

Table 6
Geometric parameters of distibine and distibene complexes

Compound	Bond lengths (Å)		Angles (°)		Conformation	Referenses
$[(CO)_5CrMe_2Sb]_2$	Sb–Sb	2.810(5)	C–Sb–C	99.18(1), 100.33(1)	Antiperiplanar (*trans*)	[45]
	Sb–Cr	2.621(4), 2.628(4)	Cr–Sb–Sb	118.37(1), 122.41(1)		
			C–Sb–Sb	96.58(1)–104.36(1)		
$RH_2SbW(CO)_5$	Sb–W	2.7568(2), 2.7564(2)	C–Sb–W	121.06, 121.9(5)	Synperiplanar	[22]
$[(CO)_5WR(H)Sb]_2$	Sb–Sb	2.8417(1)	W–Sb–Sb	123.33(4)	Anticlinal	[22]
d,l-form	Sb–W	2.7766(8)				
	Sb–Sb	2.8325(1)	W–Sb–Sb	114.01(4), 123.724(2)		
meso-form	Sb–W	2.7754(8), 2.7918(1)			Antiperiplanar (*trans*)	[22]
			C–Sb–Sb	94.1(3)		
			C–Sb–Sb	97.2(3), 102.1(3)		
RSb=SbR[W(CO)$_5$]	Sb–Sb	2.7412(1)	W–Sb–C	133.87(12), 106.01(1)	*trans*	[22]
	Sb–W	2.9494(1), 2.9913(1)	C–Sb–Sb	109.79(1)		

$R = (Me_3Si)_2CH$.

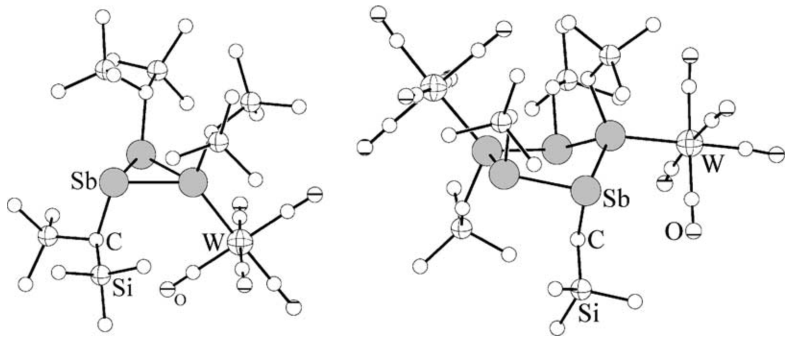

Fig. 17. Structures of *cyclo*-μ-$(RSb)_5$-Sb^1, Sb^3-$[W(CO)_5]_2$ and *cyclo*-$[(RSb)_3]W(CO)_5$ $R = (Me_3Si)_2CH$ [21,28].

In $[Me_3Si)_2CHSb]_3W(CO)_5$, the antimony ring adopts a *cis-trans*-configuration. The ring is coordinated as an η^1-ligand to the $W(CO)_5$ fragment. In the crystal there are two shorter, 2.8233, 2.8287 Å and a longer Sb–Sb bond 2.8704 Å. The Sb–Sb bond lengths are comparable with those found in $(Me_3SiCH_2Sb)_5[W(CO)_5]_2$ (2.8182–2.8417 Å). $[(Me_3Si)_2CHSb]_3W(CO)_5$ is also remarkable because NMR spectra reveal an interesting dynamic behavior at elevated temperatures (Fig. 18).

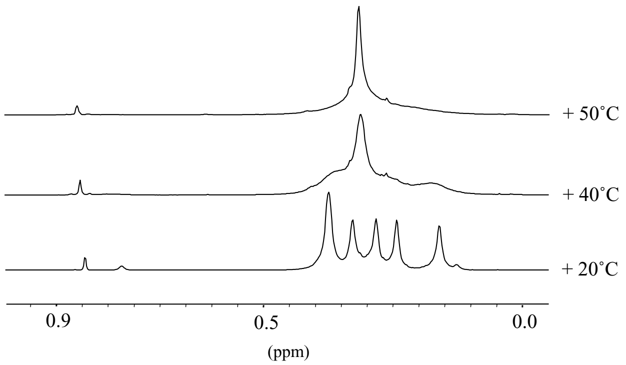

Fig. 18. ^1H NMR spectra of *cyclo*-$[(RSb)_3]W(CO)_5$ $R = (Me_3Si)_2CH$ in C_6D_6 at different temperatures [21].

The spectrum at room temperature corresponds to the molecular structure found in the crystal. It contains five singlet signals for the Me_3Si groups, one of them with double intensities, and two singlet signals for the CH groups. Above +50 °C there are two signals, one for each of the groups. These changes occur in a reversible process, that probably involves the inversion of the configuration at antimony and migration of the $W(CO)_5$ groups (or $^3\eta$ coordination (Eq. (13)).

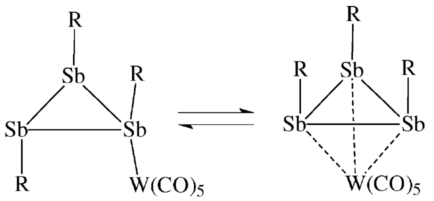

(13)

Insertion of 16-electron fragments into Sb–Sb bonds also occurs. One example is the reaction of *cyclo*-R_3Sb_3 with $Fe_2(CO)_9$ giving $R_3Sb_3Fe(CO)_4$, $R = (Me_3Si)_2CH$ [28] (Eq. (14)). The structure of this heterocycle is depicted in Fig. 19. The bonding of the R_3Sb_3 ligand to the $Fe(CO)_4$ fragment results in a folded Sb_3Fe ring. The structure of the heterocyclic complex corresponds to the isolobal homocycle *cyclo*-R_4Sb_4. The Sb–Sb bond lengths in $R_3Sb_3Fe(CO)_4$ (2.8736, 2.8581 Å) are comparable

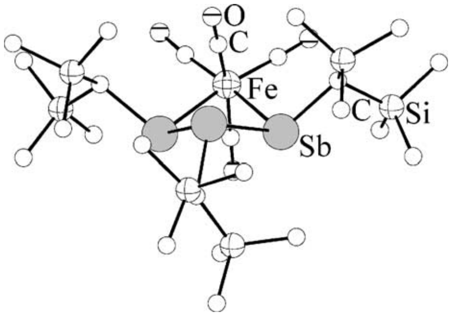

Fig. 19. Structure of *cyclo*-$[(RSb)_3]Fe(CO)_4$ $R = (Me_3Si)_2CH$ [28].

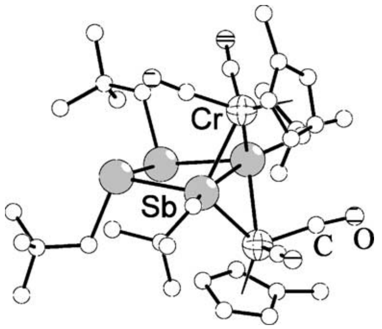

Fig. 21. Structure of $(RSb)_4[Cr(CO)_2MeC_5H_4]_2$, $R = (Me_3Si)_2CH$ [21].

with the bonds lengths (Sb–Sb, 2826–2.878 Å) found in *cyclo*-R_4Sb_4 $R = (Me_3Si)_2CH$ [27]. The Sb–Sb–Sb angle (74.95°) in $R_3Sb_3Fe(CO)_4$ is more acute than in the case of *cyclo*-R_4Sb_4, $R = (Me_3Si)_2CH$ (80.27–80.75°) [27]. The geometry around the Fe center is distorted octahedral.

$$(RSb)_3 + Fe_2(CO)_9 \xrightarrow[-Fe(CO)_5]{} R_3Sb_3Fe(CO)_4, \quad R = (Me_3Si)_2CH \qquad (14)$$

Complete degradation of the ring structure with formation of stibinidene complexes occurs in reactions of R_3Sb_3 [$R = (Me_3Si)_2CH$] with $Cp^xMn(CO)_2thf$ ($Cp^x = CH_3C_5H_4$) (Eq. (15)) or $Co_2(CO)_8$ [21]. The structures of both complexes are depicted in Fig. 20.

$$(RSb)_3 + 6Cp^xMn(CO)_2(thf) \xrightarrow[-6thf]{} 3RSb[Mn(CO)_2Cp^x]_2, \quad R = (Me_3Si)_2CH \qquad (15)$$

In $RSb[Mn(CO)_2Cp^x]_2$, the RSb ligand is bridging two $Cp^xMn(CO)_2$-fragments. The geometry around the antimony center is trigonal-planar (sum of angles at Sb 360°). The Sb–Mn bond lengths are 2.4437(10) and 2.4581(11) Å. They are shorter than the sum of covalent radii, of Sb and Mn ($\sum_{r.cov.}$ Sb, Mn = 2.82 Å).

The reaction of R_3Sb_3 $R = (Me_3Si)_2CH$ with $Co_2(CO)_8$ gives $[RSbCo(CO)_3]_2$ (Eq. (16)), an orange sensitive solid. The structure of $[RSbCo(CO)_3]_2$ consists of two pyramidal $Co(CO)_3$-fragments and two bridging *cis*-RSb-fragments, in a Sb_2Co_2-core. The bond lengths Sb–Co (2.5812(7)–2.5888(8) Å) and Co–Co (2.5964(7) Å) lie in the normal range for single bonds. The Sb–Sb distance (3.1510(7) Å) is not very much longer than a Sb–Sb single bond. $[RSbCo(CO)_3]_2$ can be described in two ways, as a bis-stibinidene complex adopting a butterfly structure with a short transanular Sb···Sb contact, or as a complex of a distibene ligand, *cis*-RSb=SbR with *side-on* coordination to two cobalt centers.

$$\tfrac{2}{3}(RSb)_3 + [Co_2(CO)_8] \xrightarrow[-2CO]{} [RSbCo(CO)_3]_2, \quad R = (Me_3Si)_2CH \qquad (16)$$

Another interesting complex, $(Me_3CCH_2Sb)_4[Cr(CO)_2Cp^x]_2$ [21] was obtained by the reaction of $(Me_3CCH_2Sb)_5$ with $[Cp^xCr(CO)_3]_2$ ($Cp^x = MeC_5H_4$) in toluene (Eq. (17)). The structure contains a $(Me_3CCH_2Sb)_4$-fragment bridging two $CrCp^x(CO)_2$-fragments (Fig. 21).

$$\tfrac{4}{5}(RSb)_5 + [Cr(CO)_3Cp^x]_2 \xrightarrow[-2CO]{} (RSb)_4[Cr(CO)_2Cp^x]_2, \quad R = Me_3CCH_2;\ Cp^x = MeC_5H_4 \qquad (17)$$

The Sb–Sb bond lengths and Sb–Sb–Sb angles in $(Me_3CCH_2Sb)_4[Cr(CO)_2Cp^x]_2$ range between 2.8322(8) and 2.9737(8) Å; 89.63(3) and 91.94(3)°. The Sb_4-core is almost planar, with a mean deviation from the best plane of 0.1493 Å. The antimony chromium bond lengths lie between 2.6749(14) and 2.7296(11) Å.

Other reaction patterns of organometallic antimony rings include substitution or removal of organo substituents. Substitution of a ^{t}Bu group by a 17 electron fragment occurs in the reaction of $^tBu_4Sb_4$ with $[Cp^xMo(CO)_3]_2$ giving $^tBu_3Sb_4[Mo(CO)_3Cp^x]$. Further substitution gives complexes with Sb_2, *cyclo*-Sb_3 or *cyclo*-Sb_5 ligands $[Cp^x(CO)_2Mo]_2Sb_2$, $Cp^x(CO)_2MoSb_3$, and $(Cp^xMo)_2Sb_5$ [1,8].

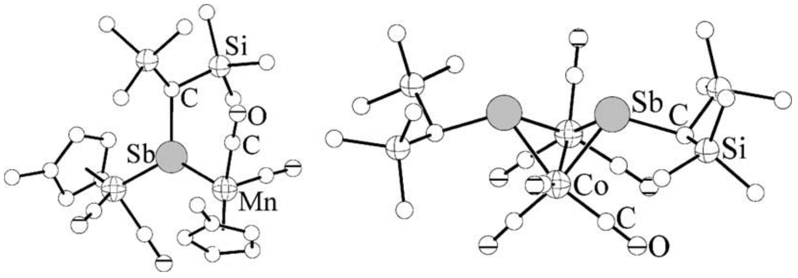

Fig. 20. Structure of $RSb[Mn(CO)_2MeC_5H_4]_2$ and $[RSbCo(CO)_3]_2$; $R = (Me_3Si)_2CH$ [21].

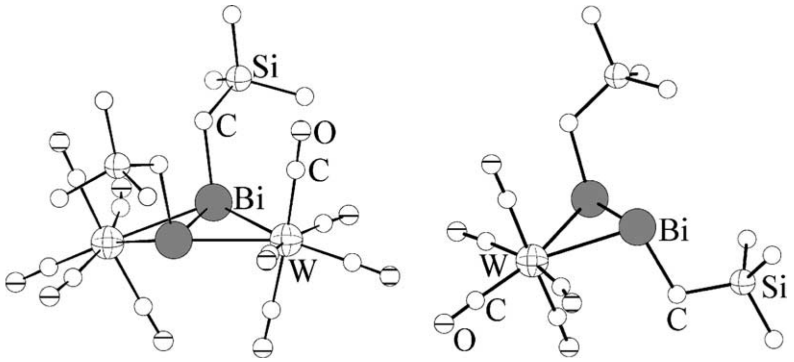

Fig. 22. Structures of [*cis*-$RBi)_2$][$W(CO)_5]_2$ and *trans*-[Rbi=BiR]$W(CO)_5$ (R = Me_3SiCH_2) [29].

The reaction patterns emerging from the study of the reactivity of cyclobismuthines with transition metals are only in some aspects analogous to cyclostibine chemistry. The main difference is that under similar conditions no complexes with lone pair donation from bismuth to a transition metal center are formed. The reactions of alkylcyclobismuthines with $W(CO)_5$thf do not lead to the coordination of the bismuth rings. Instead the rings degrade to dibismuthene ligands with *side-on* coordination through the electrons of the Bi–Bi double bond to two or one $W(CO)_5$ units.

The reaction of $(Me_3CCH_2Bi)_n$ ($n = 3, 5$) with $W(CO)_5$thf gives the dibismuthene complex [{μ-η^2-*cis*-$(Me_3CCH_2Bi)_2$}{$W(CO)_5$}$_2$] [29] (Eq. (18)). The structure of this complex (Fig. 22) consists of *cis*-dineopentyldibismuthene with a torsion angle C(1)–Bi(1)–Bi(1′)–C(1′) of 0° in a *side-on* bridging position between two $W(CO)_5$ fragments (1:2 complex). The metal core adopts a butterfly structure. The dihedral angle between the Bi_2W planes is 154.5°. The Bi–Bi bond length is 2.9799(7) Å, and the Bi–W distances are 3.1411(7) and 3.1288(7) Å. An analogous complex, [{μ-η^2-*cis*-$(Me_3SiCH_2Bi)_2$}{$W(CO)_5$}$_2$] was obtained by reaction of $(Me_3SiCH_2Bi)_n$, $n = 3, 5$ with $W(CO)_5$thf [35]. Both 1:2 dibismuthene tungsten complexes are stable only in the solid state. They decompose in solution with elimination of a $W(CO)_5$ group and formation of the *cis*- and *trans*-isomers of 1:1 complexes [28] (Eq. (19)). The crystal structure of [η^2-*trans*-$(Me_3SiCH_2Bi)_2W(CO)_5$] [29] (Fig. 22) contains a dibismuthene ligand, that is slightly distorted from planarity. The torsion angle C(1)–Bi(1)–Bi(2)–C(2) is −166.1(2)°. The dibismuthene is *side-on* coordinated to the $W(CO)_5$ fragment.

$$\frac{2}{n}\text{cyclo-}(RBi)_n + 2W(CO)_5\text{thf} \xrightarrow{-2\text{thf}} (RBi)_2[W(CO)_5]_2,$$
$$R = Me_3CCH_2,\ Me_3SiCH_2; \quad n = 3, 5 \qquad (18)$$

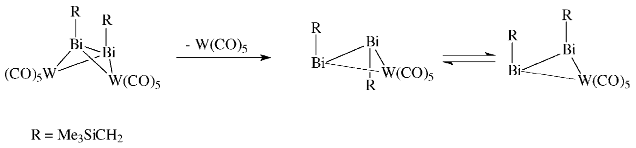

R = Me_3SiCH_2

(19)

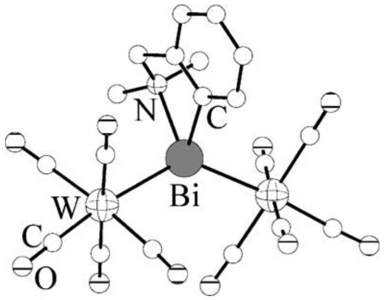

Fig. 23. Structure of $RBi[W(CO)_5]_2$, R = 2-$(Me_2NCH_2)C_6H_4$ [36].

The Bi–Bi bond in [η^2-*trans*-$(Me_3SiCH_2Bi)_2W(CO)_5$] [2.8769(5) Å] is significantly shorter than that in [{μ-η^2-*cis*-$(Me_3SiCH_2Bi)_2$}{$W(CO)_5$}$_2$] [3.003(1) Å] [35]. It is only a little longer than Bi–Bi double bonds in uncoordinated dibismuthenes [10,12].

A different reaction pattern, i.e. complete degradation of a bismuth ring system to a bismuthinidene (RBi) ligand, is observed in the reaction of [2-$(Me_2NCH_2)C_6H_4Bi]_n$, $n = 3, 4$, with $W(CO)_5$thf (Eq. (20)). Under the influence of the electron pair donation from nitrogen to bismuth the bismuthinidene complex [2-$(Me_2NCH_2)C_6H_4$]Bi[$W(CO)_5]_2$ is formed [36].

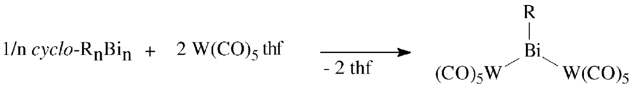

$$1/n\ cyclo\text{-}R_nBi_n + 2\ W(CO)_5\ thf \xrightarrow[-\ 2\ thf]{} (CO)_5W\text{–}Bi(R)\text{–}W(CO)_5$$

R = 2-$(Me_2NCH_2)C_6H_4$

(20)

The crystal structure of this complex (Fig. 23) consists of the organobismuth group in a bridging position between two pentacarbonyl tungsten fragments. The bismuth atom is four coordinate in an irregular trigonal pyramidal environment, with Bi–W bond lengths of 2.8248(8) and 2.8362(8) Å. The W_2BiC core is almost planar (the sum of angles around Bi is 346.53°), with the Bi atom situated only 0.5 Å above the W_2C plane. $RBi[W(CO)_5]_2$ can be described as a complex of a RBi ligand with two sp^2 orbitals containing lone pairs of electrons and an empty p-orbital at the bismuth atom. The

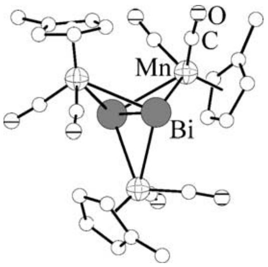

Fig. 24. Structure of $[\mu\text{-}\eta^3\text{-}Bi_2][W(CO)_5]_3$ [57].

filled orbitals are involved in the dative bonds to the tungsten atoms and the empty p orbital is accepting electron density from the amine group and the tungsten atoms. The structure is certainly also influenced by the constraints imposed by the five-membered chelate ring.

Further degradation of a cyclobismuthine with formation of Bi_2 units occurs in the reaction of *cyclo*-$(Me_3SiCH_2Bi)_n$ with $MeC_5H_4Mn(CO)_2thf$, and $Bi_2[Mn(CO)_2MeC_5H_4]_3$ a complex with the dibismuth ligand is formed [59]. This homologue of a dinitrogen complex was obtained and structurally characterized before by Huttner and co-workers [57]. The structure is depicted in Fig. 24.

11. Concluding remarks

The organometallic chemistry of compounds with Sb–Sb bonds has developed considerably during the last decades and a variety of structural types has been realised. Beginning with the large number of tetraorgano distibines, R_4Sb_2 and the series of monocycles R_nSb_n ($n = 3$–6) with known crystal structures, also more complex molecules with Sb–Sb single bonds, like the neutral species R_4Sb_8, R_6Sb_8, R_6Sb_5Cl, or the ionic compounds, $R_6Sb_3^+$, $R_4Sb_3^-$ have been synthesized. Single crystal diffractometry proved to be a very powerful method for the characterization of these compounds, which by other methods are not easily identified. A remarkable development is the synthesis and full characterization of distibenes, RSb=SbR, the first molecules with Sb–Sb double bonds. After the first studies of the coordination chemistry of Sb–Sb bonded organometallic compounds in the 1970s the field has been expanded and it was shown that antimony ligands such as distibenes, organoantimony rings and chains or “naked” Sb_2, *cyclo*-Sb_3, or *cyclo*-Sb_5 units can be derived from the distibine H(R)Sb–Sb(R)H or from cyclostibines, $(RSb)_n$.

The field of organometallic compounds with Bi–Bi bonds has also developed since the first tetraorganodibismuthine was obtained by Paneth and Loleit [58] in the 1930s. Recently, more examples of dibismuthines and also mono- and polycyclic bismuthines have been synthesized and characterized by X-ray diffraction. Emerging trends in the chemistry of cyclobismuthines reveal reactivity patterns, which are not simply extrapolations from other pnicogen analogues but reveal fundamental differences between bismuth and the lighter congeners.

Acknowledgements

Financial support by the Deutsche Forschungsgemeinschaft and the Universität Bremen is gratefully acknowledged.

References

[1] H.J. Breunig, R. Rösler, Chem. Soc. Rev. 29 (2000) 403.
[2] H.J. Breunig, R. Rösler, Coord. Chem. Rev. 163 (1997) 33, and references cited therein.
[3] H.J. Breunig, Main Group Met. Chem. 16 (1993) 143.
[4] H.J. Breunig, in: S. Patai (Ed.), The Chemistry of Organic Arsenic, Antimony and Bismuth Compounds, J. Wiley, Chichester, 1994, p. 563.
[5] H.J. Breunig, in: S. Patai (Ed.), The Chemistry of Organic Arsenic, Antimony and Bismuth Componds, J. Wiley, Chichester, 1994, p. 441.
[6] N. Tokitoh, J. Organomet. Chem. 611 (2000) 217.
[7] P.P. Power, Chem. Rev. 99 (1999) 3463.
[8] H.J. Breunig, I. Ghesner, Adv. Organomet. Chem. 49 (2003) 95.
[9] P. Pyykkö, Chem. Rev. 88 (1988) 563.
[10] B. Twamley, C.D. Sofield, M.M. Olmstead, P.P. Power, J. Am. Chem. Soc. 121 (1999) 3357.
[11] N. Tokitoh, Y. Arai, T. Sasamori, R. Okazaki, S. Nagase, H. Uekusa, Y. Ohashi, J. Am. Chem. Soc. 120 (1998) 433.
[12] N. Tokitoh, Y. Arai, R. Okazaki, S. Nagase, Science 277 (1997) 78.
[13] T. Sasamori, N. Takeda, N. Tokitoh, Chem. Commun. (2000) 1353.
[14] T. Sasamori, N. Takeda, M. Fujio, M. Rimura, S. Nagase, N. Tokitoh, Angew. Chem. 114 (2002) 147;
T. Sasamori, N. Takeda, M. Fujio, M. Rimura, S. Nagase, N. Tokitoh, Angew. Chem. Int. Ed. Engl. 41 (2002) 139.
[15] K. Issleib, B. Hamann, L. Schmidt, Z. Anorg. Allg. Chem. 339 (1965) 289.
[16] H.J. Breunig, M. Denker, K.H. Ebert, J. Organomet. Chem. 470 (1994) 87.
[17] M. Ates, H.J. Breunig, S. Gülec, W. Offermann, K. Häberle, M. Dräger, Chem. Ber. 122 (1989) 473.
[18] H.J. Breunig, M. Denker, K. Häberle, M. Dräger, T. Severengiz, Angew. Chem. 97 (1985) 62;
H.J. Breunig, M. Denker, K. Häberle, M. Dräger, T. Severengiz, Angew. Chem. Int. Ed. Engl. 24 (1985) 72.
[19] H.J. Breunig, R. Rösler, E. Lork, Organometallics 17 (1998) 5594.
[20] H.J. Breunig, W. Kanig, A. Soltani-Neshan, Polyhedron 2 (1983) 291.
[21] G. Balazs, H.J. Breunig, E. Lork, Z. Anorg. Allg. Chem. 629 (2003) 1937.
[22] G. Balázs, H.J. Breunig, E. Lork, S.A. Mason, Organometallics 22 (2003) 576.
[23] O. Mundt, G. Becker, H.J. Wessely, H.J. Breunig, H. Kischkel, Z. Anorg. Allg. Chem. 486 (1982) 70.
[24] G. Balazs, H.J. Breunig, E. Lork, Z. Anorg. Allg. Chem. 629 (2003) 637.
[25] O.M. Kekia, R.L. Jones, A.L. Rheingold, Main Group Chem. 15 (1996) 4104.
[26] T.F. Berlitz, H. Sinning, J. Lorberth, U. Müller, 1992, private communication.
[27] M. Ates, H.J. Breunig, K.H. Ebert, S. Gülec, R. Kaller, M. Dräger, Organometallics 11 (1992) 145.

[28] G. Balazs, H.J. Breunig, E. Lork, Z. Anorg. Allg. Chem. 627 (2001) 1855.
[29] L. Balázs, G. Balazs, H.J. Breunig, E. Lork, Organometallics 22 (2003) 2919.
[30] C.J. Spencer, W.N. Lipscomb, Acta Cryst. 14 (1961) 250.
[31] J.J. Dally, J. Chem. Soc. (1964) 6147.
[32] J.H. Burns, J. Waser, J. Am. Chem. Soc. 79 (1957) 859.
[33] R.L. Wells, C.-Y. Kwag, A.P. Purdy, A.T. McPhail, C.G. Pitt, Polyhedron 9 (1990) 319.
[34] H.J. Breunig, R. Rösler, E. Lork, Angew. Chem. 110 (1998) 3361; H.J. Breunig, R. Rösler, E. Lork, Angew. Chem. Int. Ed. Engl. 37 (1998) 3175.
[35] L. Balázs, H.J. Breunig, E. Lork, Angew. Chem. 114 (2002) 2411; L. Balázs, H.J. Breunig, E. Lork, Angew. Chem. Int. Ed. 41 (2002) 2309.
[36] L. Balázs, H.J. Breunig, E. Lork, C. Silvestru, Eur. J. Inorg. Chem. (2003) 1361.
[37] G. Linti, W. Köstler, Z. Anorg. Allg. Chem. 628 (2002) 65.
[38] G. Linti, W. Köstler, H. Pritzkow, Eur. J. Inorg. Chem. (2002) 2643.
[39] H.J. Huheey, Anorganische Chemie, Walter de Gruyer, Berlin, 1998, p. 1066.
[40] P.P. Power, J. Chem. Soc., Dalton Trans. (1998) 2939.
[41] A. Silvestru, H.J. Breunig, K.H. Ebert, R.J. Kaller, J. Organomet. Chem. 501 (1995) 117.
[42] A.J. Ashe III, Adv. Organomet. Chem. 30 (1990) 77.
[43] G. Balazs, H.J. Breunig, E. Lork, W. Offermann, Organometallics 20 (2001) 2666.
[44] O. Mundt, H. Riffel, G. Becker, A. Simon, Z. Naturforsch. 39b (1984) 317.
[45] A.J. Ashe III, E.G. Ludwig, J. Oleksyszyn, J.C. Hoffman, Organometallics 3 (1984) 337.
[46] K.V. Deuten, D. Rehder, Cryst. Struct. Commun. 9 (1980) 167.
[47] G. Balazs, H.J. Breunig, E. Lork, Organometallics 21 (2002) 2584.
[48] H.J. Breunig, I. Ghesner, E. Lork, Organometallics 20 (2001) 1360.
[49] H.J. Breunig, I. Ghesner, M. Ghesner, E. Lork, J. Organomet. 667 (2003) 15.
[50] H. Althaus, H.J. Breunig, E. Lork, Chem. Commun. (1999) 1971.
[51] R. Minkwitz, C. Hirsch, Z. Anorg. Allg. Chem. 625 (1999) 1672.
[52] H.J. Breunig, M.E. Ghesner, E. Lork, J. Organomet. Chem. 660 (2002) 167.
[53] R.A. Bartlett, H.V. Rasika Dias, H. Hope, B.D. Murray, M.M. Olmstead, P.P. Power, J. Am. Chem. Soc. 108 (1986) 6921.
[54] A.M. Arif, A.H. Cowley, N.C. Norman, M. Pakulski, Inorg. Chem. 25 (1986) 4836.
[55] A.H. Cowley, N.C. Norman, M. Paluski, D.L. Bricker, D.H. Russell, J. Am. Chem. Soc. 107 (1985) 8211.
[56] G. Huttner, U. Weber, O. Scheidsteger, L. Zsolnai, Angew. Chem. 94 (1982) 210;
G. Huttner, U. Weber, O. Scheidsteger, L. Zsolnai, Angew. Chem. Int. Ed. Engl. 21 (1982) 215.
[57] K. Plossl, G. Huttner, L. Zsolnai, Angew. Chem. 101 (1989) 482; K. Plossl, G. Huttner, L. Zsolnai, Angew. Chem. Int. Ed. Engl. 28 (1989) 446.
[58] F.A. Paneth, H.J. Loleit, J. Chem. Soc. (1935) 366.
[59] L. Balázs, H.J. Breunig, unpublished results.